On nucleation and the evolution of morphology in a propylene/ethylene copolymer

Y. Zhao[a], A.S. Vaughan[b],*, S.J. Sutton[c], S.G. Swingler[c]

[a]*J.J. Thomson Physical Laboratory, The University of Reading, Reading RG6 6AF, UK*
[b]*Department of Electronics and Computer Science, University of Southampton, Highfield, Southampton SO17 1BJ, UK*
[c]*National Grid, Engineering and Technology, Kelvin Avenue, Leatherhead KT22 7ST, UK*

Abstract

The morphology and crystallisation behaviour of a propylene/ethylene copolymer have been studied as a function of both crystallisation temperature and melt history, in the absence of any nucleating additives. In contrast to the previous paper, here melt temperatures were chosen to vary the number of residual lamellar fragments remaining prior to the onset of crystallisation, to permit so-called self-seeding effects to be explored. DSC results indicate that, under all circumstances, two lamellar populations develop isothermally. At sufficiently high temperatures, these are accompanied by a third quenched component. Although this general pattern of crystallisation is not qualitatively affected by the choice of self-seeding conditions, melting at 168°C (to remove self-seeding effects) does markedly reduce the proportion of primary lamellae. In all samples, TEM examination reveals the presence of two distinct lamellar types, extensive lath-like crystals and smaller, cross-hatching lamellae. The extensive laths result from primary crystallisation, whereas the cross-hatching is associated with secondary crystallisation. Quenched material is assumed to be located between individual lamellae since, where isothermal crystallisation has proceeded to completion, there is no evidence of macroscopic segregation consistent with the size of the DSC quench peak. The architecture of the lamellar aggregates, when small, is identical to the quadrites we have described previously. As the self-seeding temperature is increased, the nucleation density decreases and larger structures develop. These exhibit a number of characteristic forms, depending upon the direction in which they are viewed. Finally, when crystallisation occurs from non-seeded melts (melt temperature of 168°C), irregular spherulitic structures are seen to develop. The form of these structures is markedly influenced by the non-crystallisable fraction of the melt, which serves to suppress primary crystallisation. © 2001 Elsevier Science Ltd. All rights reserved.

Keywords: Propylene/ethylene copolymer; Self-seeded nucleation; Morphology

1. Introduction

Semi-crystalline polymers can exhibit a wide range of different morphological features, depending upon the precise composition of the system and its processing history. Of particular importance are molecular mass distribution [1], co-monomer content [2], the presence of additives [3], thermal history [4,5] and strain (both in the solid [6] and melt phases [7]). While many of these factors are exploited as general means of controlling structure and thereby properties (e.g. the improvement in the fracture toughness of polyethylene through the incorporation of short-chain branches [8]), the inclusion of additives as morphology modifiers is particularly common in conjunction with polypropylene and related copolymers. The crystallisation of propylene-based systems is unusual in two respects. First,

at the lamellar level, development of the common α-crystal form is dominated by frequent twining. This process of cross-hatching [9] results in morphologies that are based upon two sets of lamellae, which are close to orthogonal but with a common crystallographic b-axis [10]. Second, the crystallisation of polypropylene tends to involve the growth of large spherulites [11] and, as a result, the inclusion of heterogeneous nucleating additives is often a technological requirement, for example, to improve mechanical properties or to reduce optical haze [12,13]. The effectiveness of various nucleating systems is, therefore, an important practical consideration.

Nucleating efficiency values can be determined in a number of ways, and these can broadly be classified as isothermal or dynamic. Isothermally, the crystallisation half-time (or some related parameter) can be measured and compared with the equivalent quantity obtained from the polymer itself. While this is a thorough process, it is time consuming and limited to those temperatures where

* Corresponding author.
E-mail address: asv@ecs.soton.ac.uk (A.S. Vaughan).

isothermal conditions can be achieved — that is, high temperatures, above those which are likely to be technologically relevant. For both these reasons, dynamic techniques are often preferred, where the peak crystallisation temperature of the nucleated system can be measured during cooling and compared with that of the "pure" polymer. Clearly, this approach only provides a very crude measure, which is based upon a single reference point (the crystallisation temperature of the polymer itself). For this reason, Fillon et al. [14] proposed an alternative approach, in which the efficiency of a nucleating agent is compared with two dynamic reference points. These are taken to be the crystallisation temperature of the polymer, as crystallised normally, and the same polymer, but "ideally" nucleated. To produce an ideally nucleated material, it is heated to just above its melting temperature, so that a large number of residual crystal fragments remain in the melt and act as nuclei. Such techniques are commonly referred to as self-seeding or self-nucleation [15]. By comparing the crystallisation temperature of various nucleated polymers with the temperature range defined above, Fillon et al. proposed that the nucleating efficiency of various additives could each be expressed as a percentage of the "ideal". In this way, for example, a 2% addition of 4-biphenyl carboxylic acid was found to be 66% efficient, whereas 1% 2-hydroxy 3-naphthoic acid exhibited an efficiency of only 7% [14].

Whilst the concept of an ideally nucleated system is clearly a useful one, in the previous paper [16] we showed how the addition of a sorbitol clarifying additive only results in profuse nucleation when crystallisation occurs at a suitably low temperature. In this paper, we showed how the morphology changes abruptly when the crystallisation temperature exceeds 128°C, such that the observed etched surfaces become extremely rough. This change in lamellar texture was interpreted in terms of a marked reduction in the nucleating effectiveness of the clarifier at high temperatures (i.e. at 128°C and above), which consequently permits the formation of relatively large aggregates of lamellae (quadrites). This transition implies that the sorbitol has a sharply defined effective range, when incorporated into propylene-based polymers. Accompanying the formation of quadrites, appreciable molecular segregation was observed and, in concert, these two processes affected certain macroscopic physical parameters.

In this paper, we explore nucleation effects in the same copolymer, but in the absence of any nucleating additives. Here the nucleation event is associated with the conformations of the polymer itself within the melt, rather than the presence of the clarifier. This was undertaken with three specific objectives in mind.

1. To examine high temperature quadrite morphologies further, by varying the nucleation density in a manner that is not possible in the clarified systems described previously.
2. In view of the pronounced temperature dependence of the nucleating efficiency of the clarifying additive, to explore the extent to which self-seeded samples can be considered to be ideally nucleated.
3. To investigate the extent to which the initial nucleation event has any influence upon subsequent growth.

2. Experimental

2.1. Materials and sample preparation

All the results reported here were obtained from the propylene/ethylene copolymer, Novolen 3240NC (BASF), which is the unclarified analogue of the Novolen 3200MC (BASF) used in our previous study. Gel permeation chromatography (GPC) gave average molecular mass values of $M_w = 2.2 \times 10^5$ and $M_n = 5.9 \times 10^4$ and, using the infrared procedures described by Baker et al. [17], the copolymer was found to contain a total ethylene co-monomer content of 3.5%.

Samples for self-seeded crystallisation were initially prepared by pressing the pelletised polymer between a slide and a cover slip on a Koffler hot bench at 165°C. They were then transferred to a Mettler FP52 hot-stage at 210°C, held for 3 min under nitrogen flow, and quenched on a cold metal surface, to provide a reference material with a standard thermal history. Samples for study were then prepared from this reference, by first heating to the desired melt temperature in the Mettler hot-stage. This enabled the number of remnant crystal nuclei to be varied. Specimens were then immediately cooled to the crystallisation temperature and held for the required time. After crystallisation was complete, all samples were finally quenched into ice/water.

2.2. Characterisation methods

Optical examination between crossed polars was performed during crystallisation in the hot-stage and following quenching. All other sample characterisation techniques were as described in the preceding paper and, therefore, only brief notes are included here. Samples for transmission electron microscopy (TEM) were prepared using permanganic etching followed by two stage, indirect replication [18–20]. The material's thermal behaviour was investigated using a Perkin–Elmer DSC-2C differential scanning calorimeter (DSC) after calibration with high-purity indium. All data acquisition and analysis were performed by computer.

3. Results and discussion

3.1. Thermal behaviour

Fig. 1 shows the DSC melting behaviour of the unclarified propylene/ethylene copolymer, as a function of crystallisation temperature (T_c). In all cases, the sample was heated
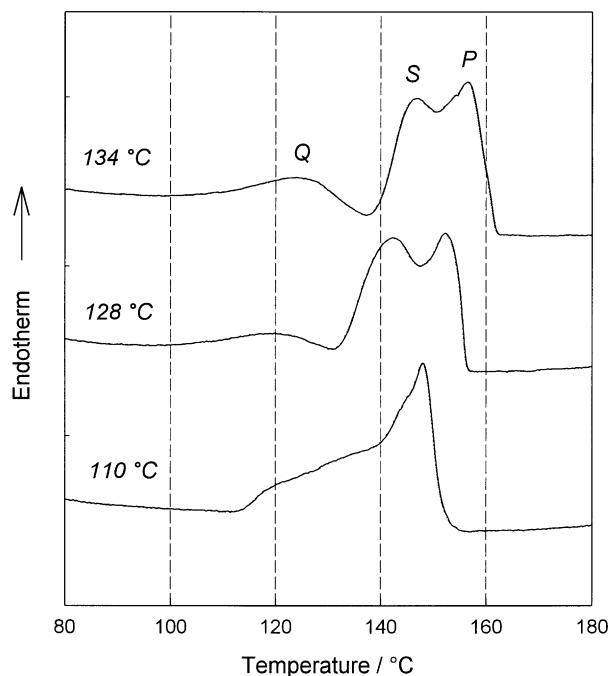
Fig. 1. DSC melting behaviour of the propylene/ethylene copolymer as a function of crystallisation temperature. All samples were nucleated by self-seeding at 160°C before being crystallised to completion at the indicated temperatures: the DSC scan rate was 10K/min.
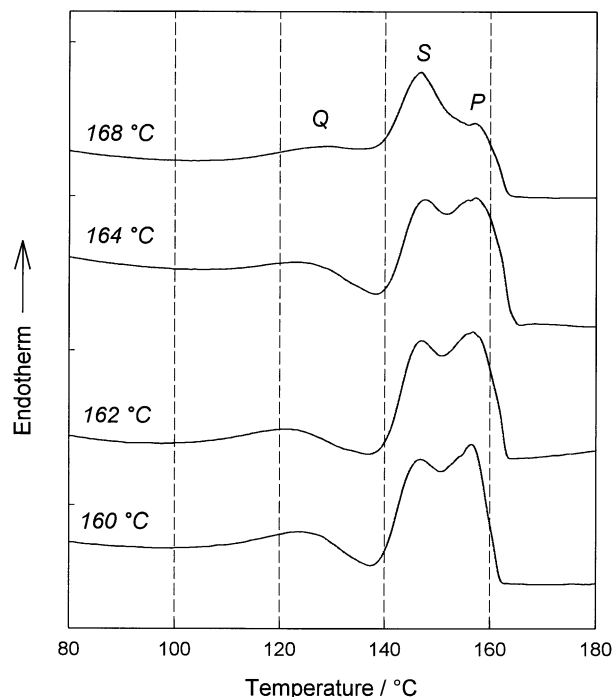

Fig. 2. DSC melting behaviour of the propylene/ethylene copolymer as a function of melt history. Each sample was heated to the indicated temperature before being crystallised to completion at 134°C: the DSC scan rate was 10K/min.

to a self-seeding temperature of 160°C prior to crystallisation and then melted at a scan rate of 10K/min. Multiple peaks can be seen in all the traces. When $T_c \geq 128$°C, three peaks are present that are marked P, S and Q with decreasing temperature. At lower crystallisation temperatures, 110°C in Fig. 1, peak Q is absent. These results are qualitatively in line with published DSC data obtained from comparable propylene/ethylene copolymers [21,22] and are identical to the traces described previously for the equivalent clarified system [16]. Thus, peaks P and S should both be associated with isothermal crystallisation. Peak P results from the fusion of crystallites that develop during primary crystallisation, whilst peak S is associated with some secondary crystallisation process. Conversely, peak Q is again a consequence of fractionation of the ethylene-rich segments and their subsequent crystallisation on quenching.

The effect of the self-seeding temperature on melting behaviour is shown in Fig. 2. All these traces were obtained from samples that were heated to different temperatures and then crystallised to completion at 134°C. As above, all these data were similarly recorded at a scan rate of 10K/min. From these, it is evident that a change in melt temperature does not qualitatively affect the subsequent crystallisation process, since Fig. 2 again shows clear evidence of primary, secondary and quenched lamellae. However, although an invariant proportion of the material is unable to crystallise at 134°C, it is clear that the relative magnitude of peak P decreases markedly when the self-seeding temperature is raised from 164 to 168°C. The form of the trace obtained

from the 168°C sample is consistent with Feng and Hay's [23] data obtained from a comparable material slow-cooled from the melt. Thus, heating to 168°C appears sufficient to melt the specimen fully, whereas at lower melt temperatures, self-seeding effects will be observed.

3.2. Optical textures

Fig. 3a and b shows the optical appearance of two samples, which were melted at 168 and 162°C, respectively, before being crystallised at 134°C. After heating to the higher temperature, mature spherulitic structures are found to develop. These exhibit characteristic circular projections, particularly when the sample is not crystallised to completion, and are equivalent to structures we have shown previously [16]: that is, these objects are comparable to the textures that develop when higher melt temperatures are employed, indicating that, at 168°C and above, self-seeding effects are negligible. The internal extinction patterns are complex, due to spatial variations in the extent of cross-hatching. In polypropylene, spherulites have been characterised on the basis of their optical appearance and are termed negative (radial lamellae dominate), positive (tangential cross-hatching lamellae dominate) or mixed (neither dominate throughout the spherulite) [24–26]. Fig. 3a is representative of so-called mixed spherulites, which therefore indicates the presence of appreciable
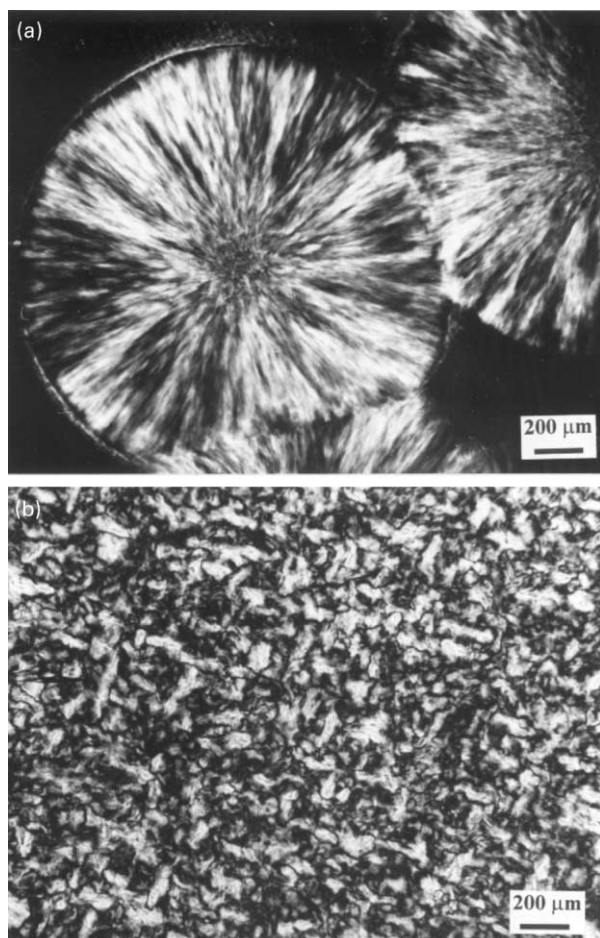
Fig. 3. Transmission optical micrographs (crossed polars) showing samples crystallised to completion at 134°C, after being melted at (a) 168°C; and (b) 162°C.
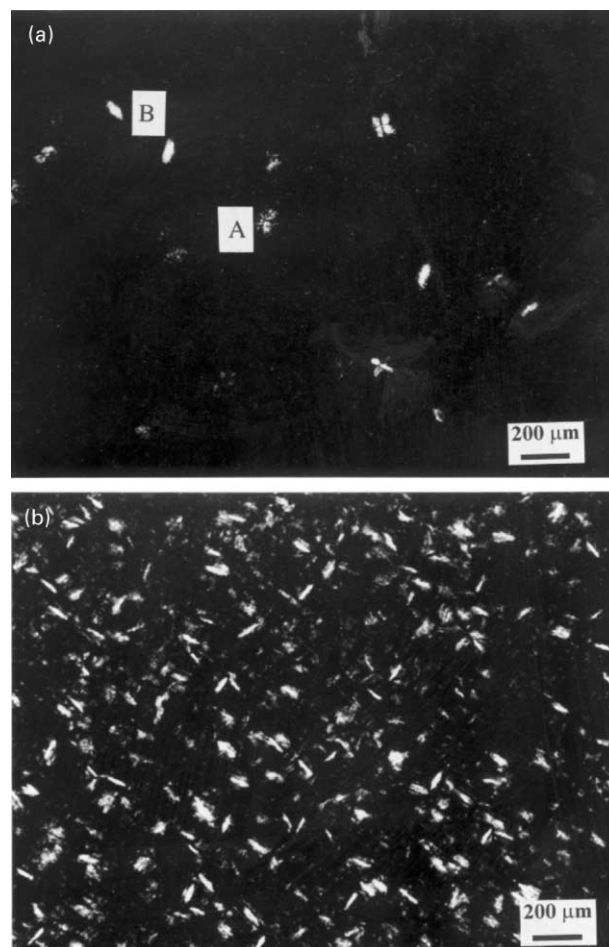

Fig. 4. Optical micrographs showing samples partially crystallised (1 h at 134°C) and then quenched into ice/water: (a) melted by heating to 168°C; and (b) melted by heating to 162°C.

quantities of both radial lamellae and cross-hatching but the comprehensive dominance of neither.

Self-seeding by heating to 162°C results in a very different optical texture. From Fig. 3b, it is clear that the nucleation density is dramatically increased and, in addition, the form of the constituent objects appears very different from the well-defined spherulites described above. Although there do not appear to be any mature spherulites in this sample, impingement and superposition of different objects along the light path can result in extinction patterns that are not easily interpreted. Consequently, so as more clearly to reveal the constituent morphological forms, other samples were crystallised isothermally following different melting treatments, but quenched prior to impingement.

Fig. 4 contains optical micrographs showing samples that were crystallised for 1 h at 134°C, after heating to 168°C (Fig. 4a) and 162°C (Fig. 4b). From Fig. 4a, the morphology can be described in terms of two characteristic optical textures. Several objects appear weakly birefringent, approximately circular in projection and exhibit a typical mixed optical texture (e.g. at A). Such objects can, therefore, easily be related to the large spherulites previously

shown in Fig. 3a. In addition, there are also other objects that appear radially elongated and uniformly bright (e.g. at B). Insertion of a λ-plate between the crossed polars reveals that these objects are positively birefringent — that is, the major refractive index is oriented along the long axis of the structure. Similar observations have been reported in polypropylene [25,26], where they are best explained in terms of an idealised quadrite. As described in the previous paper [16], such objects contain two nearly orthogonal sets of lath-like lamellar crystals. Thus, when viewed along the common b-axis of both cross-hatched populations, the structure appears rectangular in form and weakly birefringent. When viewed along any orthogonal axis, the object appears much more elongated, due to the inherent lath-like crystal habit of polypropylene, and much more strongly birefringent. In this projection, the observed birefringence results from the effective axial orientation of the molecules within the cross-hatched lamellar populations that make up the structure. Thus, the variation in optical texture described above is entirely consistent with immature spherulitic forms based upon near-orthogonal sets of lamellae.

After self-seeding by partially melting the sample at

162°C, an identical crystallisation procedure (1 h at 134°C) results in a much more profusely nucleated sample. However, otherwise, the individual lamellar aggregates appear entirely analogous to those described above. Thus, contrary to our DSC results where systematic variations were seen with melt temperature, provided objects of identical size are examined, the gross morphological form does not appear to be affected by the initial crystallisation procedure. Nevertheless, in order to explore variations in internal lamellar texture further, a range of samples was examined in the TEM.

3.3. Lamellar morphologies

Crystallisation after melting at 160°C. Electron micrographs of samples crystallised at different temperatures are shown in Figs. 5 and 6; all these samples were initially melted at 160°C in order to preserve many crystal nuclei. Fig. 5a shows a low magnification image of a sample that was crystallised at 128°C, in which a rough etched surface can be seen containing a number of apparently linear
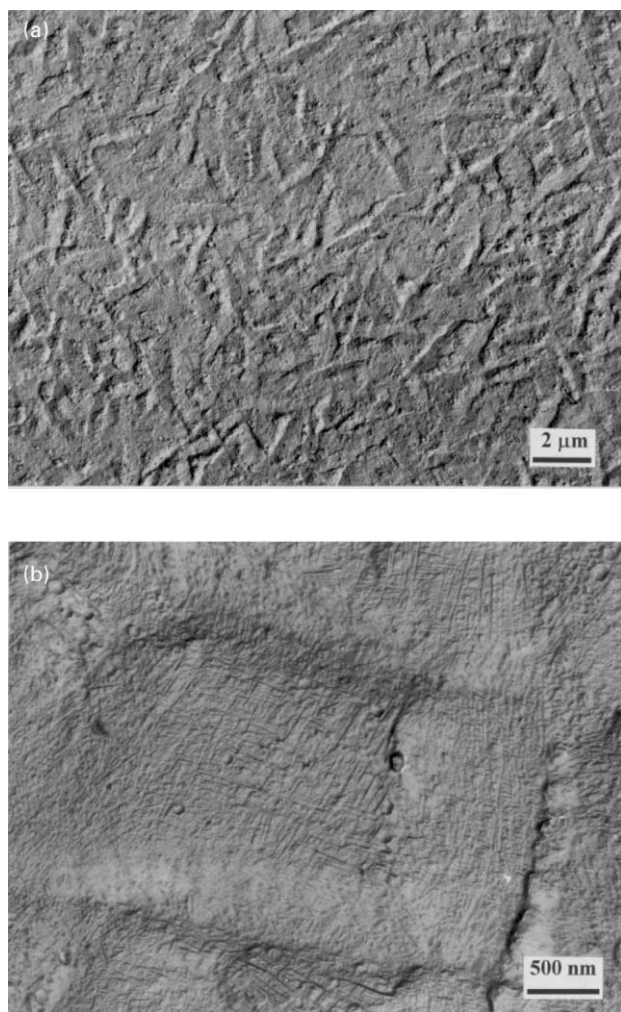
Fig. 5. Electron micrographs of samples crystallised at (a) 128°C; and (b) 134°C. Both samples were nucleated by self-seeding at 160°C.
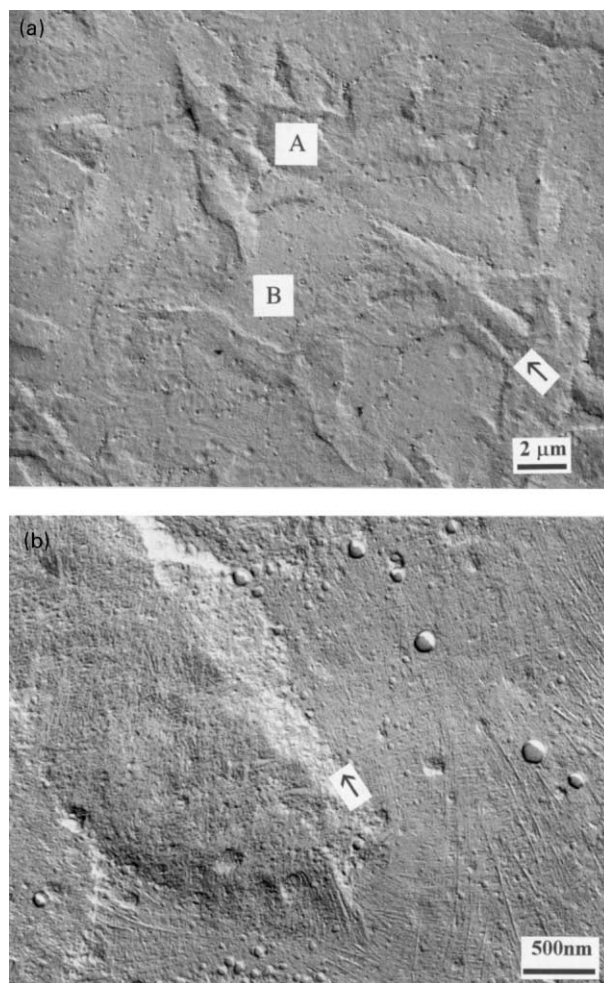
Fig. 6. Electron micrographs of a sample crystallised at 110°C following nucleation by self-seeding at 160°C.

structures. This is identical to the morphologies seen in the clarified copolymer when, similarly, crystallised in its high temperature range (at 128°C and above). However, when viewed at higher magnifications, the origin of these structural features is clearly revealed, particularly when the crystallisation temperature is raised to 134°C. Fig. 5b shows such a sample. Throughout this micrograph, lamellar crystals of the order of 1 μm in length can be seen edge-on, which are separated from one another by smaller cross-hatched structures. At the centre, the rectangular outline of a quadrite is clear. These results, obtained where nucleation densities are moderately high, are therefore in complete agreement with those obtained from equivalent samples containing the clarifying agent (cf. Fig. 5a here and Ref. [16, Fig. 6]), when similarly crystallised at high temperatures. Consequently, the surface texture shown in Fig. 5a is, again, a result of the etched plane intersecting with many different, randomly oriented quadrites. When viewed along the crystallographic *b*-axis, such objects appear close to square; when viewed along any orthogonal direction, they appear elongated.

At lower crystallisation temperatures, the overall morphological form becomes substantially modified. Fig. 6 shows a sample that was melted at 160°C and then crystallised at 110°C (i.e. within the temperature range where the sorbitol results in massive nucleation [16]). In Fig. 6a, many pronounced surface features can be seen, such as those at A, together with areas in which few clear structural elements can be identified (e.g. at B). Examination at a higher magnification reveals that this is again a consequence of the etched surface containing many objects that are being viewed in a range of orientations. Objects in two different orientations can be seen impinging, where arrowed. At this temperature, more extensive spherulitic development has occurred, such that clear spherulitic characteristics can be identified. At the bottom right of Fig. 6b, for example, extensive lamellar splay is evident and, as a consequence, it is possible to describe the morphology in terms of extensive *radial* primary lamellae and less well developed *tangential* cross-hatching. Also, the presence of the gross surface structures suggests that lamellar branching is not just occurring about the *b*-axis (cf. that arrowed in Fig. 6a and the linear surface features seen in Fig. 5a). White and Bassett [27] showed that when polypropylene lamellae grow away from row nuclei, their inherent lath-like habit would result in the development of extensive gaps between neighbouring laths. The size of these gaps would, in the absence of other processes, increase with increasing radial distance. That such gaps are generally filled indicates that a number of branching processes are operative in the system. Within the context of this work, this means that branching does not only occur within the initial plane of a quadrite but, also, perpendicular to it. In this way, spherical objects can develop from planar precursors.

From the above results, it is evident that crystallisation at 110°C results in immature spherulitic structures that are much larger than the quadrites seen at 134°C. This necessarily implies that, in comparison with the 134°C sample, the effective nucleation density is lower at the lower crystallisation temperature. This is contrary to the notion that, following self-seeding, nucleation occurs upon the remnant crystal fragments since, then, the number of nucleation sites should depend only upon the self-seeding temperature. Whilst it would appear that self-seeding is more effective at high crystallisation temperatures, our previous work has shown that the sorbitol clarifier is far more effective at the lower temperatures seen in practical applications. Thus, although self-seeding can result in a higher temperature crystallisation exotherm in a DSC cooling scan, morphologically, describing self-seeded specimens as "ideally nucleated" is unwarranted.

Effect of melt temperature on crystallisation at 134°C. Fig. 7 contains micrographs of a sample that was nucleated at 162°C, crystallised at 134°C for 1 h and then quenched. Under these conditions, lamellar aggregates develop, which continue the theme described above. The nucleation density is reduced and, consequently, much more extensive objects are able to develop. In this specimen, isothermal crystallisation was terminated prior to completion, such that quenched regions can very occasionally be seen between neighbouring objects. However, in view of the appreciable molecular fraction that, from DSC data, is unable to crystallise at 134°C, the rarity of distinct quenched zones must indicate that this fraction is, primarily, located between individual lamellae. In Fig. 7a, a number of randomly oriented objects can be seen and, as a consequence of this, the overall lamellar texture appears rather complex. Consider, therefore, only the region between A and the two arrows, which defines a sector of a spherulitic structure. At the growth tips (between the two arrows, for example), individual radial lamellae can be seen, which are separated from one another by quenched material. Since these crystals must have developed prior to in-filling by cross-hatching, they must correspond to the primary population revealed by DSC. Some distance from the periphery of the object, clear cross-hatching can be seen between the dominant lamellae. Finally, at the finest scale, there is also some evidence of quenched structures between the isothermal lamellae. Quenched material is, however, not only evident at the very tips of the structure, as indicated by the arrowed zones that lie well within the overall envelope of the object. In these regions, isothermal growth has been suppressed, since the constituent molecular fraction is only able to crystallise on quenching. Such features provide the first evidence for the accumulation of a defective non-crystallisable fraction (peak Q in Fig. 1) serving to modify morphological evolution.

Elsewhere, in Fig. 7a, the simple and rather conventional pattern of crystallisation described above is not so apparent. At B, for example, lamellae are oriented in such a way as to make interpretation of the morphology much more difficult. Nevertheless, the detailed lamellar texture is entirely consistent with the DSC data presented in Figs. 1 and 2 and apparent spatial variations are, again, best explained in terms of impinging objects oriented in various ways with respect to the etched surface.

Fig. 7b shows a low-magnification micrograph of the above sample, in which a large, extended structure can be seen. The dominant feature of this is the clear splay (arrowed) that can be seen, even when the lamellae are viewed along the chain axis: that is, the lamellae are branching in a manner that is inconsistent with lattice continuity [27], in order to facilitate growth outside the plane of the initial quadrite. Such objects are, therefore, immature spherulites in that they exhibit all the characteristics necessary for the eventual attainment of a spherical envelope.

Further increases in melt temperature result in further reductions in nucleation density and the development of increasingly spherulitic objects. Fig. 8 shows a sample that was melted completely by heating to 168°C, crystallised at 134°C for 3 h and then quenched (cf. Fig. 3a). From micrographs such as this, it is not possible to obtain any quantitative estimates of the relative quantities of dominant
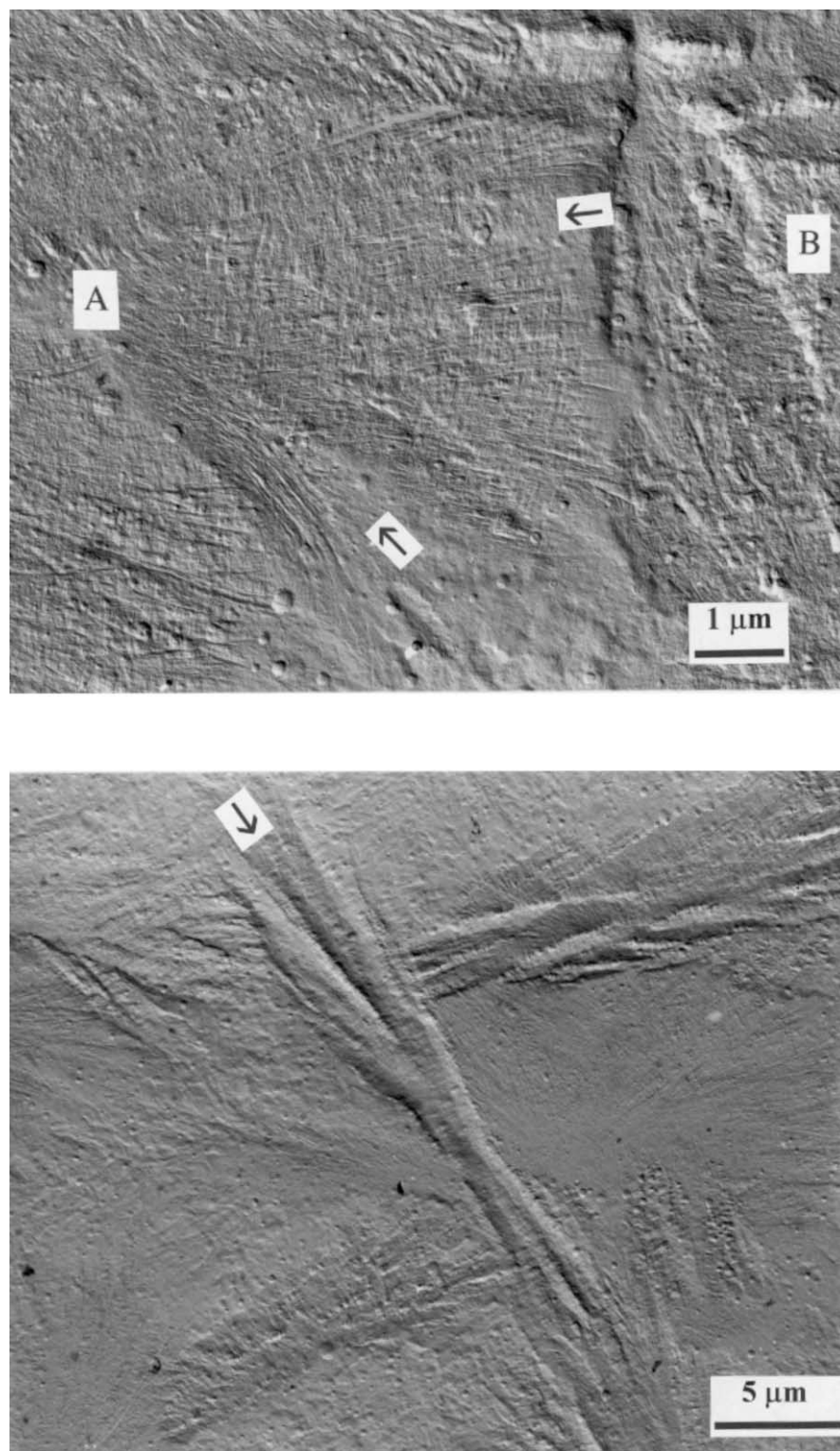
Fig. 7. Electron micrographs of a sample nucleated by self-seeding at 162°C, then crystallised at 134°C for 1 h before being quenched.

(primary) and subsidiary (secondary, cross-hatching) lamellae. However, there are a number of features that suggest that, quantitatively, the process of crystallisation is now rather different from that discussed above. In this case, the overall outline of the structure (Fig. 8a) is highly reminiscent of the transverse views through row structures described by White and Bassett [27]. Indeed, at A in Fig. 8b, radial lath-like lamellae are viewed close to flat-on
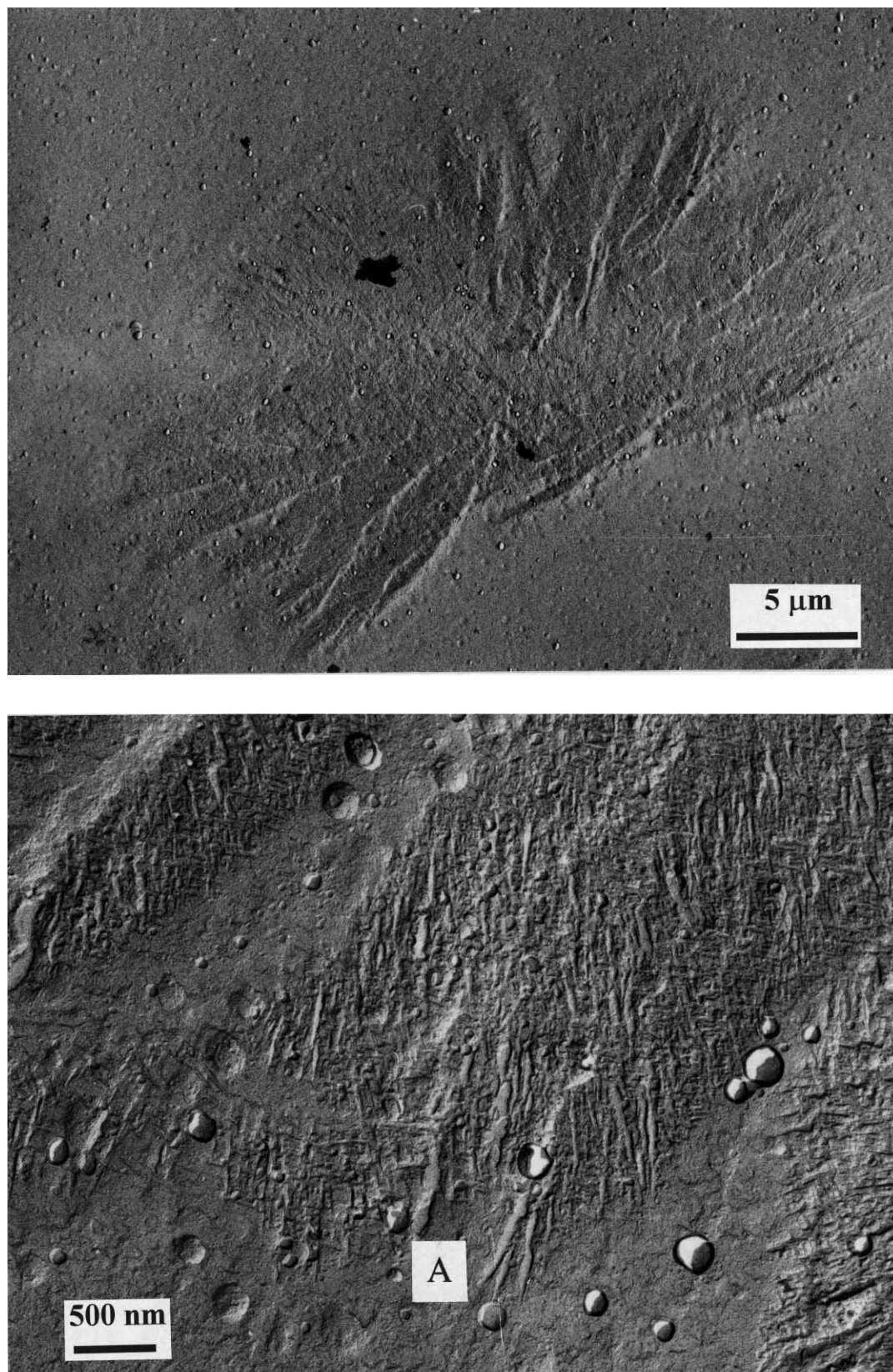
Fig. 8. Electron micrographs showing a sample that was completely melted by heating to 168°C, crystallised at 134°C for 3 h and, finally, quenched.

(i.e. along their *c*-axis). The fact that development has occurred outside the plane defined by the initial quadrite again demonstrates the propensity for lamellae to splay via whatever mechanism permits efficient, space-filling crystallisation. The rather irregular outline is also significant and is, we believe, associated with the variation in melting behaviour shown in Fig. 2.

Irregular spherulitic envelopes are often associated with growth in the presence of non-crystallisable impurities [28,29]. In polypropylene, it has been shown that such features can be associated with the tacticity of the material [27] such that, in systems that contain a substantial atactic fraction, growth occurs via radially extended units separated by gaps. Presumably, these gaps contain material that is too defective to crystallise under isothermal conditions. Here, the material is a copolymer of propylene and ethylene and, as indicated by DSC, contains a fraction that is too high in ethylene to crystallise at 134°C. Thus, the presence of extensive quenched zones well within the body of a spherulite may, similarly, indicate that the process of crystallisation is being perturbed by the accumulation of a defective fraction at the periphery of the object. The existence of such material at the interface would, per se, exert more of an impact upon the formation of high melting dominant lamellae than upon the lower melting crystals, which develop as part of the secondary crystallisation process. In isotactic polystyrene, for example, the addition of atactic material to the melt reduces the spherulite growth rate [30] and results in the formation of a more open interface, where the spacing between neighbouring dominant lamellae is increased [31]. Conversely, where nucleation occurs more uniformly, large spherulites like that shown in Fig. 8a do not have sufficient space to develop and, consequently, molecular segregation cannot occur on such a macroscopic scale.

The above analysis indicates that structural dimensions can influence the crystallisation process, particularly where the melt contains an appreciable non-crystallisable fraction. Such concepts have been exploited in many studies of crystallisation [32–34]. All the DSC data shown in Fig. 2 were obtained from samples that had been crystallised to completion at 134°C. However, although the crystallisation temperature remained constant, it is the self-seeding temperature that defines the nucleation density and, therefore, the ultimate scale of the evolving structures. Clearly, from Fig. 3, the objects that develop when this material is melted at 168°C and crystallised to completion at 134°C are very different from those that form at an identical temperature after melting at 162°C, even though, when small, they are the same. Thus, we propose that the observed variation in DSC behaviour is due to size effects. Where the accumulation of a defective fraction occurs at the interface of growing spherulites, this subsequently serves to perturb the formation of dominant lamellae more than the later forming subsidiary cross-hatching. Where the nucleation density is much higher, segregation on the scale of spherulitic dimensions does not occur and, therefore, primary crystallisation appears, relatively, enhanced.

4. Conclusions

A variety of morphological forms has been identified in this copolymer, as a result of variations in melt and crystallisation conditions. These range from immature quadrites to extensive spherulites. However, the internal texture of all these structures is based upon two distinct isothermal lamellar populations. Extensive lath-like lamellae that, in spherulitic structures, are radially oriented, and smaller interstitial cross-hatching lamellae. The lath-like lamellae result from primary crystallisation whereas cross-hatching is associated with secondary crystallisation. Quantitatively, the relative magnitude of each population can vary in response to prior melt history. When extensive structures develop in the presence of an appreciable non-crystallisable molecular fraction, spherulitic envelopes are perturbed, interfacial periodicities increase and, consequently, the overall fraction of primary (dominant) lamellae is reduced.

Contrary to our expectations, it would appear that the effectiveness of self-seeded nucleation is markedly dependent upon the chosen crystallisation temperature. Nucleation densities are highest at high crystallisation temperatures whereas, where growth occurs more rapidly, the observed nucleation densities appear appreciably reduced. Since it is difficult to envisage a mechanism by which potential nucleation sites may become inactive at lower temperatures, the above results more reasonably imply that these potential nuclei can be characterised by a range of crystallisation induction times.

The behaviour described above is significantly different from that of the clarified analogue that we described previously. Self-seeding and the addition of the sorbitol both result in similar nucleation densities at temperatures between 128 and 134°C. However, whilst self-seeded nucleation densities decrease with crystallisation temperature, the nucleating efficiency of the clarifier increases dramatically below 128°C. Thus, self-seeding may well result in the formation of a higher temperature crystallisation exotherm than an equivalent clarified material, when both are similarly cooled from the melt in the DSC. Nevertheless, from a morphological viewpoint, it is equally clear that self-seeded specimens cannot be considered to be ideally nucleated, particularly at the low crystallisation temperatures that are encountered technologically.

References

[1] Bassett DC, Hodge AM. Proc R Soc Lond A 1981;377:25.
[2] Voigt-Martin IG, Mandelkern L. In: Cheremisinoff NP, editor.

Handbook of polymer science and technology, vol. 3. New York: Marcel Dekker, 1989. p. 1.

[3] Kopp S, Wittmann JC, Lotz B. Polymer 1994;35:908.

[4] Overbergh N, Berghmans H, Reynaers H. J Polym Sci: Polym Phys Ed 1976;14:1177.

[5] Fillon B, Wittmann JC, Lotz B, Thierry A. J Polym Sci, Part B: Polym Phys Ed 1993;31:1383.

[6] Butler MF, Donald AM. J Mater Sci 1997;32:3675.

[7] Pople JA, Mitchell GR, Sutton SJ, Vaughan AS, Chai CK. Polymer 1999;40:2769.

[8] Mirabella FM, Westphal SP, Fernando PL, Ford EA, Williams JG. J Polym Sci, Part B: Polym Phys Ed 1988;26:1995.

[9] Khoury F. J Res Nat Bur Stand 1966;70A:29.

[10] Padden FJ, Keith HD. J Appl Phys 1973;44:1217.

[11] Padden FJ, Keith HD. J Appl Phys 1959;30:1479.

[12] Gahleitner M, Wolfschwenger J, Bachner C, Bernreitner K, Neissl W. J Appl Polym Sci 1996;61:649.

[13] Sterzynski T, Lambla M, Crozier H, Thomas M. Adv Polym Technol 1994;13:25.

[14] Fillon B, Thierry A, Lotz B, Wittmann JC. J Therm Anal 1994;42:721.

[15] Blundell DJ, Keller A, Kovacs AJ. J Polym Sci, Part B: Polym Lett 1966;4:481.

[16] Zhao Y, Vaughan AS, Sutton SJ, Swingler SG. Polymer, 2001;42: 6587.

[17] Baker BB, Bonesteel JK, Keating MY. Thermochim Acta 1990;166:53.

[18] Olley RH, Hodge AM, Bassett DC. J Polym Sci: Polym Phys Ed 1979;17:627.

[19] Olley RH, Bassett DC. Polymer 1982;32:1707.

[20] Willison JHM, Rowe AJ. Replica shadowing and freeze-etching techniques. Amsterdam: North Holland, 1980.

[21] Laihonen S, Gedde UW, Werner PE, Martinez-Salazar J. Polymer 1997;38:361.

[22] Laihonen S, Gedde UW, Werner PE, Westdahl M, Jääskeläinen P, Martinez-Salazar J. Polymer 1997;38:371.

[23] Feng Y, Hay JN. Polymer 1998;39:6589.

[24] Norton DR, Keller A. Polymer 1985;26:704.

[25] Olley RH, Bassett DC. Polymer 1989;30:399.

[26] Binsbergen FL, de Lange BGM. Polymer 1968;9:23.

[27] White HM, Bassett DC. Polymer 1998;39:3211.

[28] Braun D, Jacobs M, Hellmann GP. Polymer 1994;35:706.

[29] Abo el Maaty MI, Bassett DC, Olley RH, Jääskeläinen P. Macromolecules 1998;31:7800.

[30] Yeh GSY, Lambert SL. J Polym Sci: Part A-2 1972;10:1183.

[31] Vaughan AS. Polymer 1992;33:2513.

[32] Keith HD, Padden FJ. J Polym Sci, Part B: Polym Phys 1987;25: 2265.

[33] Jasnow D. Superlattices Microstruct 1987;3:581.

[34] Seetharaman V, Eshelman MA, Trivedi R. Acta Metall 1988;36:1175.